Volume 229, number 2, 367–371 FEB 05676 March 1988

Resonance Raman evidence for an unusually strong exogenous ligand–metal bond in a monomeric nitrosyl manganese hemoglobin

Shun-Hua Lin, Nai-Teng Yu and Klaus Gersonde*

School of Chemistry, Georgia Institute of Technology, Atlanta, GA 30332, USA and **Hauptabteilung Medizintechnik, Fraunhofer-Institut für zerstörungsfreie Prüfverfahren and Fachrichtung Medizintechnik, Universität des Saarlandes, D-6600 Saarbrücken, FRG*

Received 21 January 1988

Resonance Raman spectroscopy has been employed to determine the vibrational modes of monomeric nitrosyl manganese *Chironomus thummi thummi* hemoglobin (CTT IV). This insect hemoglobin has no distal histidine. By applying various isotope-labeled nitric oxides ($^{14}N^{16}O$, $^{15}N^{16}O$, $^{14}N^{18}O$), we have identified the Mn^{II}-NO stretching mode at 628 cm^{-1}, the Mn^{II}-N-O bending mode at 574 cm^{-1} and the N-O stretching mode at 1735 cm^{-1}. The results suggest a strong Mn^{II}–NO bond and a weak N–O bond. The vinyl group substitution does not influence the $\nu(Mn^{II}\text{-}NO)$, $\delta(Mn^{II}\text{-}N\text{-}O)$ and $\nu(N\text{–}O)$ vibrations. The Mn^{II}-NO stretching frequency is insensitive to distal histidine interactions with NO, whereas the N–O stretching frequency is sensitive. Nitric oxide also binds to Met manganese CTT IV to form an $Mn^{III}\cdot NO$ complex which undergoes a slow but complete autoreduction resulting in the $Mn^{II}\cdot NO$ species. In manganese meso-IX CTT IV, the $Mn^{III}\cdot NO$ $Mn^{II}\cdot NO$ conversion alters the intensities of the porphyrin ring modes at 342, 360, 1587 and 1598 cm^{-1}, but shifts the frequencies at 1504 and 1633 cm^{-1} (in $Mn^{III}\cdot NO$) to 1497 and 1630 cm^{-1} (in $Mn^{II}\cdot NO$), respectively. The unshifted marker line at 1378 cm^{-1} reflects the fact that the π^* electron densities of the porphyrin ring are the same in the two complexes.

Resonance Raman spectroscopy; Hemoglobin; Nitrosyl manganese hemoglobin; Metal-ligand vibrational mode; *(Chironomus thummi thummi)*

1. INTRODUCTION

Resonance Raman spectroscopy provides direct information on properties of the metal–ligand bond in hemoglobins [1–3]. Of particular interest is the bond strength between metal and axial ligands, as the nature of these bonds plays an important role in the allosteric control of ligand binding in hemoglobins. In general, the bond strength is correlated with the bond length: the stronger the bond, the shorter the bond length. Furthermore, the bond length is related to the force constant according to Badger's rule [4]. The force constant in turn determines the bond stretching frequency. Here, we measure the Mn-NO stretching frequency and compare it with the frequencies of Fe^{II}-CO stretching [5] and Fe^{III}-CN^- stretching [6] in the monomeric hemoglobin CTT IV from the insect *Chironomus thummi thummi*. CTT IV is a very simple allosteric system, which exhibits a Bohr effect with a missing distal histidine [7–10]. We selected the three above-mentioned complexes as they show linear axial ligand-metal moieties. Furthermore, resonance Raman data of these hemoglobin complexes are compared with those of corresponding model compounds: $Mn^{II}(TPP)(MPip)(NO)$, 1.644 Å [11]; $Fe^{II}(TPP)(Py)(CO)$, 1.770 Å [12]; $Fe^{III}(TPP)(Py)(CN^-)$, 1.908 Å [11,13], for which the lengths of the metal–ligand bonds are known from X-ray structure analysis.

In this series of complexes the bond length increases with decreasing metal-ligand stretching frequency. Hence, the Mn^{II}–NO bond is the strongest

Correspondence address: K. Gersonde (*present address*), Fraunhofer Institut für zerstörungsfreie Prüfverfahren, Ensheimer Str. 48, D-6670 St. Ingbert, FRG or N.-T. Yu, School of Chemistry, Georgia Institute of Technology, Atlanta, GA 30332, USA

Published by Elsevier Science Publishers B.V. (Biomedical Division)
00145793/88/$3.50

and shortest among these mentioned complexes. This is also true for the corresponding CTT IV complexes. The Mn–NO bond stretching frequency is found to be insensitive to distal histidine interactions with NO. In contrast, the N-O stretching frequency, which indicates a weak N–O bond, is sensitive to distal histidine interactions. Both vibrational modes are insensitive to porphyrin side group substitutions. This study of nitrosyl manganese CTT IV, in particular the comparison with other isoelectric systems, enhances our understanding of subtle variations in heme metal–ligand bonding, associated with electron rearrangements.

2. MATERIALS AND METHODS

The monomeric hemoglobin CTT IV from *C. thummi thummi* was purified as described [14,15]. Manganese proto- and mesoporphyrin-IX were prepared according to standard methods [16]. Preparation of globin [17] and reconstitution [5,15,17] of CTT IV with manganese protoheme-IX and manganese mesoheme-IX, respectively, were carried out as described.

The nitrosyl complexes of manganese CTT IV were prepared as follows: a very small amount of sodium dithionite (~0.5 mg) or ascorbic acid was placed in a cylindrical quartz Raman cell. After the cell had been sealed, evacuated and flushed with pure N_2, nitric oxide gas was introduced into the cell. Then the degassed Met manganese CTT IV solution (≈80 μM in 0.2 M Tris, Bis-Tris or citrate-phosphate buffer) was added via a gas-tight syringe. $^{14}N^{16}O$ gas was obtained from Matheson Gas Products (Morrow, GA) and $^{15}N^{16}O$ gas (99 atom% ^{15}N) from Prochem US Service (Summit, NJ). The $^{14}N^{18}O$ complex was prepared in a similar manner, except that the $^{14}N^{18}O$ gas was generated by reducing potassium nitrite ($K^{14}N^{18}O_2$, Stohler Isotope Chemicals, 90 atom% ^{18}O) with ascorbic acid in the upper chamber of the Raman cell.

Raman spectra were recorded with the highly sensitive multichannel laser Raman system described in [19]. The 413.1 nm line of the krypton ion laser (Spectra Physics 171-01) was employed as excitation source. The power was approx. 15 mW at the sample. The scattered light was collected at a geometry of 90°. To eliminate photodissociation, the sample was spun throughout the measurements. All spectra were collected at room temperature, unsmoothed, and calibrated by standard compounds.

3. RESULTS AND DISCUSSION

3.1. *Assignment of Mn-NO stretching and Mn-N-O bending vibrations in nitrosyl manganese CTT IV: Indication for an unusually strong Mn–NO bond*

In fig.1 we present the resonance Raman spectra (200–750 cm^{-1} spectral region) of nitrosyl manganese meso-IX CTT IV at pH 9.4 for $^{14}N^{16}O$ (A), $^{15}N^{16}O$ (B), and $^{14}N^{18}O$ (C). Two isotope-sensitive lines are clearly identified in the spectrum of the $^{14}N^{16}O$ complex at 573 and 628 cm^{-1}. The 573 cm^{-1} line shifts to 562 cm^{-1} ($^{15}N^{16}O$ complex) and 569 cm^{-1} ($^{14}N^{18}O$ complex). The 628 cm^{-1} line shifts to 623 cm^{-1} ($^{15}N^{16}O$ complex) and 613 cm^{-1} ($^{14}N^{18}O$ complex). The 573 cm^{-1} mode exhibits a zig-zag ligand isotope shift: decrease ($^{15}N^{16}O$) ⟶ increase ($^{14}N^{18}O$). Hence, this mode is the Mn-N-O bending mode. The 628 cm^{-1} line shows a monotonic decrease in frequency with increasing ligand isotope mass. Therefore, this line has to be assigned to the Mn-NO stretching vibration. In fig.1 we also display the low-frequency spectra of nitrosyl manganese proto-IX CTT IV for $^{14}N^{16}O$ (D) and $^{15}N^{16}O$ (E). The Mn-NO stretching and Mn-N-O bending, already assigned for the meso-IX CTT IV complex, occur at the same

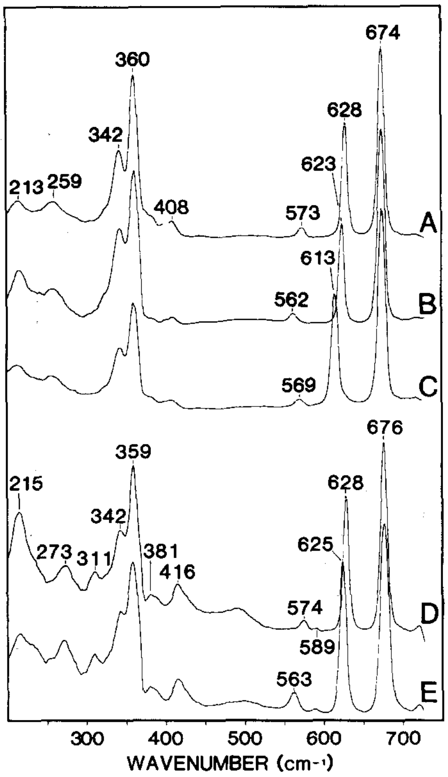

Fig.1. Effect of ligand isotope exchange on the 200–750 cm^{-1} region of the resonance Raman spectra of nitrosyl manganese meso-IX CTT IV (A, $^{14}N^{16}O$; B, $^{15}N^{16}O$; C, $^{14}N^{18}O$) and proto-IX CTT IV (D, $^{14}N^{16}O$; E, $^{15}N^{16}O$) at pH 9.4.

frequencies in the spectra of the corresponding proto-IX CTT IV complexes.

The nearly identical frequencies of the Mn-NO stretching and Mn-N-O bending modes in meso-IX and proto-IX CTT IV, respectively, reveal that the Mn–NO bond is not affected by the electron-donating or -withdrawing properties of the porphyrin side groups (replacement of vinyls in proto-IX CTT IV by ethyls results in meso-IX CTT IV). In contrast, EPR results on oxy cobalt and nitrosyl CTTs indicated an influence of those side groups of the porphyrin on the hyperfine structures, which were interpreted as indicators of influence on the central atom–axial ligand bonds [17]. Whereas EPR reflects only the distribution of the unpaired electron, the resonance Raman vibrational frequencies are the measure of the metal–ligand bond strength to which both s and p bonding contribute. Hence, hyperfine constants in EPR spectra are not necessarily a measure of metal–ligand bond strength. No influence of substituents in position 2 and 4 of the porphyrin was also reported for the Fe–CO bond [5].

The ν(Mn-NO) and δ(M-N-O) in the monomeric insect hemoglobin CTT IV are practically the same in the corresponding myoglobin complex [20], although myoglobin has a distal histidine, whereas CTT IV does not. In contrast, the influence of the distal histidine on the metal–ligand bond has been demonstrated for monomeric cobalt-nitrosyl hemoglobins [21]. An important difference between these two types of complexes is that the Mn-NO moiety is linear [1], whereas the Co-NO moiety is bent [1]. The strong Mn–NO bond may not be easily affected by the relatively weak distal histidine-NO interaction. Therefore, Mn-NO complexes in different hemoglobins show nearly the same Mn-NO stretching frequency [20]. The ~628 cm^{-1} Mn-NO stretching frequency is the highest metal-ligand stretching frequency observed to date for diatomic ligands: Fe-CO at ~500 cm^{-1}, Co-NO at ~570 cm^{-1}, Co-O_2 at 535 cm^{-1}, Fe^{II}-NO at ~554 cm^{-1}, Fe^{III}-NO at ~595 cm^{-1} and Fe^{III}-CN^- at ~452 cm^{-1}. Now, we compare only the metal-ligand frequencies of those complexes which exhibit linear exogenous ligand-metal geometry (Mn^{II}-NO, Fe^{II}-CO, Fe^{III}-CN^-). To eliminate being misled by mass effects, we calculated the metal–ligand bond stretching frequency on the basis of corrected mass normalized to the Mn-NO system. We then obtain for Fe^{II}-CO 490 cm^{-1} and for Fe^{III}-CN^- 434 cm^{-1}. These frequency numbers correlate with the force constant which is highest for the Mn–NO bond. Indeed, the bond distances determined by X-ray structural analysis for corresponding model compounds correlate with the stretching frequencies of the metal–ligand bond: Mn^{II}(TPP)(MPip)(NO), 1644 Å, 630 cm^{-1}; Fe^{II}(TPP)(Py)(CO), 1.770 Å, 487 cm^{-1}; Fe^{III}(TPP)(Py)(CN^-), 1.908 Å, 451 cm^{-1}. Although X-ray data for the nitrosyl complex of manganese CTT IV are not available, we believe, in correspondence to the model compounds, that bond length and stretching frequency correlate in the same way in the CTT IV complexes. This comparison indicates that the Mn–NO bond is strongest and hence the shortest.

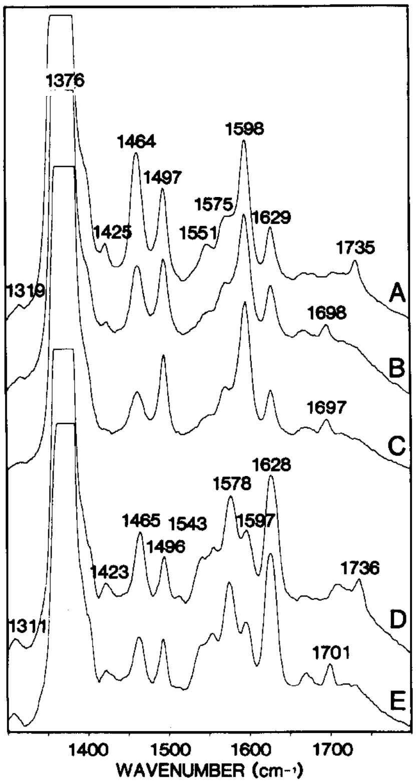

Fig.2. Effect of ligand isotope exchange on the 1300–1800 cm^{-1} region of the resonance Raman spectra of nitrosyl manganese meso-IX CTT IV (A, $^{14}N^{16}O$; B, $^{15}N^{16}O$; C, $^{14}N^{18}O$) and proto-IX CTT IV (D, $^{14}N^{16}O$; E, $^{15}N^{16}O$) at pH 9.4.

3.2. *Sensitivity of N-O stretching vibration to distal histidine-nitrosyl interaction*

Fig.2 displays the effect of nitric oxide isotope exchange on the high-frequency region (1300–1800 cm^{-1}) of the resonance Raman spectra of nitrosyl manganese CTT IV at pH 9.4. We identify the N-O stretching vibration at 1735 cm^{-1} for the ^{14}N^{16}O complex of manganese meso-IX CTT IV. This frequency is shifted to 1698 cm^{-1} (^{15}N^{16}O complex) and 1697 cm^{-1} (^{14}N^{18}O complex).

These frequency shifts resemble the shift pattern observed for the C-O stretching frequencies in carbonmonoxy CTT III. Here, the C-O stretching frequency shifts from 1960 cm^{-1} (^{12}C^{16}O complex) to 1918 cm^{-1} (^{13}C^{16}O complex) and 1918 cm^{-1} (^{12}C^{18}O complex) [22]. The small differences in stretching frequencies between ^{15}N-^{16}O and ^{14}N-^{18}O as well as ^{13}C-^{16}O and ^{12}C-^{18}O may indicate the anharmonic nature of these oscillators. The stretching frequency of N-O is 220 cm^{-1} lower than that of C-O, indicating that the N–O bond is weaker than the C–O bond. It should be noted that the observed 1735 cm^{-1} N-O stretching frequency is identical with that in the Mn(II)proto-IX-dimethyl ester (piperidine)(NO) model complex [20]. In both cases no distal histidine-NO interaction is present. However, in nitrosyl manganese myoglobin a 23 cm^{-1} shift to lower frequency was observed [20] indicating distal histidine-NO interaction. Hence, the N-O stretching in the nitrosyl manganese system and the Co-NO stretching in cobalt nitrosyl systems are sensitive monitors of distal histidine-NO interaction [21].

3.3. *Formation of Mn^{III}·NO complex and its spontaneous conversion to Mn^{II}·NO complex*

In fig.3 we display four spectra (200–700 cm^{-1}) taken at different time intervals after the addition of NO to Mn^{III} meso-IX CTT IV in the absence of other reducing agents. The most dramatic changes from (a) (10 min) to (d) (300 min) are reversal of the relative intensities at 342 and 360 cm^{-1}, and the intensity increases at 573 and 628 cm^{-1} due to the Mn^{II}-N-O bending and Mn^{II}-NO stretching, respectively. The spectrum shown in fig.3d is indistinguishable from that in fig.1A, representing the nitrosyl complex of Mn^{II} meso-IX CTT IV. The spectral features in fig.3a, different from those of Mn^{III} meso-IX CTT IV without NO (not shown), are characteristic of Mn^{III}·NO complex except the weak 628 cm^{-1} line indicating the initial fast formation of Mn^{II}·NO species. Thus, it appears that nitric oxide also binds to Mn^{III}, exhibiting a spontaneous Mn^{III}·NO ⟶ Mn^{II}·NO autoreduction. This is analogous to the well-known phenomenon observed with NO binding to ferric and ferrous hemoproteins [23].

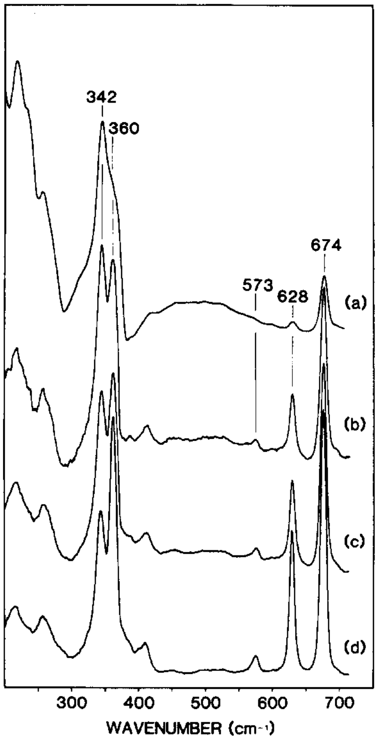

Fig.3. Time-dependent resonance Raman spectra (200–700 cm^{-1}) in the conversion of Mn^{III}·NO to Mn^{II}·NO in manganese meso-IX CTT IV at pH 9.4. (a) 10 min, (b) 150 min, (c) 200 min, (d) 300 min.

Although the Fe^{III}-NO stretching and Fe^{III}-N-O bending have been observed at 595 and 573 cm^{-1} (sperm whale myoglobin) and 604 and 574 cm^{-1} (horseradish peroxidase), respectively, we have not detected the Mn^{III}-NO stretching and Mn^{III}-N-O bending modes.

In the high-frequency region (1300–1700 cm^{-1}) spectra (not shown), we observed no frequency change at 1378 cm^{-1} in the course of Mn^{III}·NO ⟶ Mn^{II}·NO conversion. The 1378 cm^{-1} mode is the indicator of the π^* electron density of the porphyrin ring [1]. This means that there is no detectable concentration of the Mn^{II}·NO intermediate species. The difference in charge between the two complexes is absorbed by the NO ligand and the proximal histidine without affecting the π^* electron density of the porphyrin macrocycle [23]. However, the porphyrin ring modes at 1504 and 1633 cm^{-1} (in $Mn^{III} \cdot NO$) are shifted to 1497 and 1630 cm^{-1} (in $Mn^{II} \cdot NO$). In addition, we observed a large intensity decrease at 1587 cm^{-1} and an increase at 1598 cm^{-1}.

4. CONCLUSION

In three linear complexes of a monomeric insect hemoglobin (Fe^{III}-CN^-, Fe^{II}-CO and Mn^{II}-NO) the metal–ligand bond stretching frequency is highest for the Mn^{II}-NO complex indicating the strongest Mn^{II}–NO bond.

Whereas the N-O stretching frequency is sensitive to distal histidine-nitrosyl interaction, the Mn-NO stretching vibration is not.

Nitric oxide binds to Met manganese meso-IX CTT IV to form an $Mn^{III} \cdot NO$ complex which exhibits a slow, but complete autoreduction to the $Mn^{II} \cdot NO$ species.

Acknowledgements: The work was supported by the National Institutes of Health grant GM 18894 (N.-T.Y.), the Fonds der Chemischen Industrie (K.G.) and the Medizinische Biophysik eV (K.G.). We express our thanks to Miss Sigrid Engels for valuable technical assistance.

REFERENCES

[1] Yu, N.-T. (1986) Methods Enzymol. 130, 350–409.

[2] Spiro, T.G. (1983) in: Iron Porphyrins (Lever, A.B.P. and Fray, H.B. eds) pp.89–159, Addison-Wesley, Reading, MA.

[3] Rousseau, D.L. and Ondrias, M.R. (1983) Annu. Rev. Biophys. Bioeng. 12, 351–380.

[4] Herschblack, D.R. and Laurie, V.W. (1961) J. Chem. Phys. 35, 458–463.

[5] Gersonde, K., Kerr, E.A., Yu, N.-T., Parish, D.W. and Smith, K.M. (1986) J. Biol. Chem. 261, 8678–8685.

[6] Gersonde, K., Yu, N.-T., Kerr, E.A., Smith, K.M. and Parish, D.W. (1987) J. Mol. Biol. 194, 545–556.

[7] Buse, G., Steffens, G.J., Braunitzer, G. and Steer, W. (1979) Hoppe-Seyler's Z. Physiol. Chem. 360, 89–97.

[8] Huber, R., Epp, O., Steigemann, W. and Formanek, H. (1971) Eur. J. Biochem. 19, 42–50.

[9] Steigemann, W. and Weber, E. (1979) J. Mol. Biol. 127, 309–338.

[10] Pfetschinger, J., Plagens, H. and Braunitzer, G. (1981) Hoppe-Seyler's Z. Physiol. Chem. 362, 539–547.

[11] Piciulo, P.L., Rupprecht, G. and Scheidt, W.R. (1974) J. Am. Chem. Soc. 96, 5293–5299.

[12] Peng, S.M. and Ibers, J.A. (1976) J. Am. Chem. Soc. 98, 8032–8038.

[13] Scheidt, W.R., Lee, Y.J., Luangdilok, W., Haller, K.J., Auzai, K. and Hatano, K. (1983) Inorg. Chem. 22, 1516–1524.

[14] Gersonde, K., Sick, H., Wollmer, A. and Buse, G. (1972) Eur. J. Biochem. 25, 181–189.

[15] La Mar, G.N., Anderson, R.R., Chacko, V.P. and Gersonde, K. (1983) Eur. J. Biochem. 136, 161–166.

[16] Fuhrhop, J.H. and Smith, K.M. (1975) in: Porphyrins and Metalloporphyrins (Smith, K.M. ed.) p.797, Elsevier, Amsterdam, New York.

[17] Gersonde, K., Twilfer, H. and Overkamp, M. (1982) Biophys. Struct. Mech. 8, 189–211.

[18] Overkamp, M., Twilfer, H. and Gersonde, K. (1976) Z. Naturforsch. 31c, 524–533.

[19] Yu, N.-T. and Srivastava, R.B. (1980) J. Raman Spectrosc. 9, 166–171.

[20] Parthasarathi, N. and Spiro, T.G. (1987) Inorg. Chem. 26, 2280–2282.

[21] Yu, N.-T., Thompson, H.M., Mizukami, H. and Gersonde, K. (1986) Eur. J. Biochem. 159, 129–132.

[22] Yu, N.-T., Benko, B., Kerr, E.A. and Gersonde, K. (1984) Proc. Natl. Acad. Sci. USA 81, 5106–5110.

[23] Benko, B. and Yu, N.-T. (1983) Proc. Natl. Acad. Sci. USA 80, 7042–7046.